applied optics

In situ time-series monitoring of collagen fibers produced by standing-cultured osteoblasts using a second-harmonic-generation microscope

EIJI HASE,[1] OKI MATSUBARA,[1] TAKEO MINAMIKAWA,[2] KATSUYA SATO,[2] AND TAKESHI YASUI[2,*]

[1]Graduate School of Advanced Technology and Science, Tokushima University, 2-1 Minami-Josanjima, Tokushima 770-8506, Japan
[2]Institute of Technology and Science, Tokushima University, 2-1 Minami-Josanjima, Tokushima 770-8506, Japan
*Corresponding author: yasui.takeshi@tokushima-u.ac.jp

Received 24 December 2015; revised 18 March 2016; accepted 18 March 2016; posted 18 March 2016 (Doc. ID 256429); published 15 April 2016

In bone tissue engineering and regeneration, there is a considerable need for an unstained method of monitoring collagen fibers produced by osteoblasts. This is because collagen fibers play an important role as a bone matrix and continuous monitoring of their temporal dynamics is important in clarifying the organization process toward forming bone tissue. In the work described here, using a second-harmonic-generation (SHG) microscope, we performed *in situ* time-series monitoring of collagen fibers produced by cultured osteoblasts without the need for staining. Use of the 19 fs near-infrared pulsed light enables us to visualize the temporal dynamics in a thin layer of collagen fibers produced by a single layer of osteoblasts in high-contrast SHG images. While the collagen fibers were produced and stored inside the osteoblasts at an early stage of culturing, the network structure of collagen fibers was formed and locally condensed at a late stage. Furthermore, we extracted a quantitative parameter of collagen maturity degree in the cultured sample by use of image analysis based on a two-dimensional Fourier transform of the SHG image. The proposed method will be useful for *in situ* quality and quantity control of collagen fibers in bone tissue engineering and regeneration.

OCIS codes: (180.4315) Nonlinear microscopy; (170.3880) Medical and biological imaging; (190.4160) Multiharmonic generation; (170.6930) Tissue.

http://dx.doi.org/10.1364/AO.55.003261

1. INTRODUCTION

Bone is the tissue that functions as a pivotal of the human body during motion. Therefore, bone pain, deformities, and fractures reduce quality of life significantly. However, since the metabolism of bone tissue is quite slow compared with other tissues, it is difficult for the elderly to heal the damaged bone or increase a sufficient amount of bone during a short period. Therefore, there is a considerable need for bone tissue engineering and regeneration to locally replace damaged bone in the elderly [1,2].

Bone formation and regeneration in tissue engineering proceed via the following three steps. First, osteoblasts are differentiated and induced from induced pluripotent stem cells or mesenchymal stem cells. Second, osteoblasts produce collagen fibers while increasing in number. Third, mineral is deposited between the collagen fibers. Laboratory techniques for achieving the first step have already been established [3,4], and bone tissue engineering is now in the stage of the second and third steps. In these two steps, it is important to monitor the density and structure of collagen fibers because collagen fibers play an important role in constructing bone tissue as an extracellular matrix and the structural maturity of them, namely, collagen maturity, is related to bone mineralization.

Staining procedures have been widely used to selectively visualize collagen fibers in histology [5]. However, such procedures cannot be used for continuously monitoring the temporal dynamics of collagen fibers *in situ* during the culturing period due to the invasiveness of the staining procedure and the damage it causes to cells. If the distribution of collagen fibers could be visualized without the need for staining, *in situ* time-series monitoring of collagen dynamics during the culturing period would become possible. This would be useful for studying how collagen fibers behave during the second and third steps, namely, the organization process toward forming bone tissue.

Second-harmonic-generation (SHG) microscopy is a promising tool for *in situ* observation of collagen fibers in tissues without the need for staining [6]. This microscopy has high selectivity and good image contrast to collagen molecules as well as high spatial resolution, optical three-dimensional (3D) sectioning, minimal invasiveness, and moderate penetration. Therefore, it has been widely used for visualization of collagen

fibers in native tissues, such as skin [7], tendon [8], cornea [9], bone [10], and cartilage [11]. Furthermore, there are a few reports in applying SHG microscopy for the tissue engineering using fibroblast [12,13]. However, there have been no attempts to use SHG microscopy in the field of the bone tissue engineering using osteoblasts.

In the work described here, we constructed an SHG microscope using 110 fs and 19 fs near-infrared pulsed light, and compared SHG images of collagen fibers produced by cultured osteoblasts. Then, we visualized the temporal evolution of collagen fibers produced by standing-cultured osteoblasts during a culturing period of 4 weeks *in situ*. Finally, we perform image analysis of the SHG image based on the two-dimensional Fourier transform (2D-FT) to extract a quantitative parameter for the maturity degree of collagen fibers in the standing-cultured osteoblast samples.

2. MATERIALS AND METHODS

A. Samples

We used the mouse osteoblast cell line MC3T3-E1, which was provided by the RIKEN-BRC through the National Bio-Resource Project of the Ministry of Education, Culture, Sports, Science, and Technology (MEXT), Japan. The cells were cultured with α-MEM medium (Nacalai Tesque Co. Ltd.) to which was added 10% fetal bovine serum until the cultured cell concentration reached 80% confluent. We used a chamber made of silicone rubber (STREX Inc.) for cell culturing. The chamber was sterilized at 120°C for 20 min with an autoclave, and its surface was then coated with fibronectin solution (Wako Pure Chemical Industries, Ltd.) for 6 h to enhance the cell adhesion on the culture surface. Then the chamber was rinsed twice with Dulbecco's phosphate buffered saline. After the cells were seeded onto the chamber, they were cultured in the medium with an osteoblast-inducing reagent. This medium was an α-MEM medium to which was added 1% ascorbic acid, 0.2% hydrocortisone, and 2% β-glycerophosphate. For sterilization, we also added 1% penicillin and streptomycin solutions (100 U/ml and 100 μg/ml, respectively). We performed a standing culture of the cells for one, two, three, and four weeks. A single layer of osteoblasts adhered onto the bottom of the chamber produced a thin layer of collagen fibers (typical thickness <10 μm) for the culturing periods.

To confirm the production of collagen fibers by the standing-cultured osteoblasts, we applied the staining procedure using Sirius Red with the samples [14]. Sirius Red stains both the collagen fiber and the nuclear pink. The staining procedure was applied to each of the samples cultured for different periods. Figures 1(a)–1(e) show stained images of the standing-cultured osteoblast samples at 0 day, 1 week, 2 weeks, 3 weeks, and 4 weeks, respectively, after starting the standing culture (image size = 1 mm by 1 mm). In the sample cultured for 0 day, only osteoblasts should be stained with light pink because of no production of collagen fibers immediately after starting the standing culture [see Fig. 1(a)]. In the sample cultured for 1 week, the pink color became deeper due to the increased number of osteoblasts and the production of collagen fibers [see Fig. 1(b)]. However, it is not clear how much collagen fibers were produced. In the sample cultured for 2 weeks, a gradation of deep pink and light pink was observed [see Fig. 1(c)]. Since the osteoblasts were already confluent at 1 week after starting the standing culture, the gradation is mainly due to increased density of collagen fiber rather than the increased number of osteoblasts. In other words, osteoblasts produced dense collagen in some regions. In the sample cultured for 3 weeks, the gradation became clearer, and the pink color in dense collagen regions became deeper [see Fig. 1(d)]. In the sample cultured for 4 weeks in Fig. 1(e), there was no significant difference of the stained image compared with the sample cultured for 3 weeks, implying that the production of the collagen fibers was almost saturated. In this way, we confirmed the production of collagen fibers in the sample.

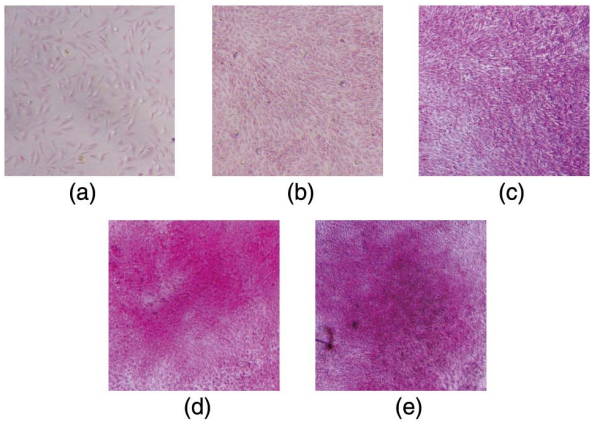

Fig. 1. Sirius-Red-stained images of collagen fibers produced in the standing-cultured osteoblast samples at (a) 0 day, (b) 1 week, (c) 2 weeks, (d) 3 weeks, and (e) 4 weeks after starting the standing culture. Image size is 1 mm by 1 mm. The collagen fibers and the osteoblasts were stained pink in this staining procedure.

B. SHG Microscope

Figure 2 shows the experimental setup of the SHG microscope. Here we used a 110 fs and 19 fs near-infrared pulsed light for SHG imaging. The 110 fs pulsed light at a wavelength of 780 nm was obtained by a frequency-doubled mode-locked erbium-doped fiber laser (FD-ML-ErF, Toptica, FFS. SYS-SHG;

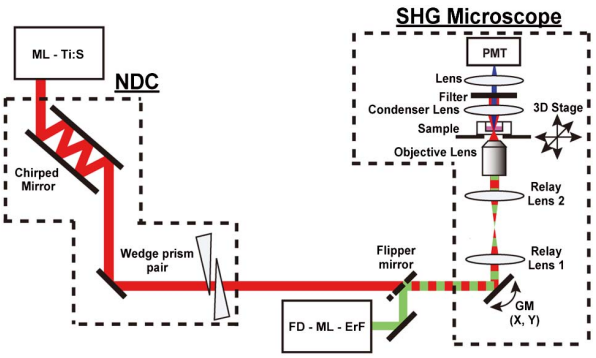

Fig. 2. Experimental setup of the SHG microscope. ML-TiS, 10 fs, 787 nm mode-locked Ti:sapphire laser; NDC, negative dispersion controller; FD-ML-ErF, 110 fs, 775 nm frequency-doubled mode-locked erbium-doped fiber laser; GM, galvanometer mirror; PMT, photon-counting photomultiplier.

spectral bandwidth=10 nm, repetition frequency=100 MHz). The pulse duration at the focal point of an objective lens was measured by a two-photon-fluorescence interferometric autocorrelator [15]. We confirmed that the pulse duration was almost the same as that at the exit window of the laser cavity (110 fs). On the other hand, the 19 fs pulsed light was achieved at the focal point by precise dispersion control of an ultrashort mode-locked Ti:sapphire laser light (ML-Ti:S, FEMTOLASERS Produktions GmbH, Femtosource Scientific Pro; pulse duration = 10 fs, center wavelength = 787 nm, spectral bandwidth = 103 nm, repetition frequency = 81.8 MHz) with an external negative dispersion controller (NDC, FEMTOLASERS Produktions GmbH, MOSAIC PRO V), composed of a negatively chirped mirror pair (group delay dispersion = −900 to −6270 fs^2) and a positively chirped wedge prism pair (group delay dispersion = +50.8 to +356 fs^2).

After selecting either 110 fs pulsed light or the 19 fs one by a flipper mirror, the laser beam was focused onto the sample with an objective lens (Olympus Corp., LUMPlanFI/IR; magnification = 60, NA = 0.90, working distance = 2 mm, water immersion) and its focal point was two-dimensionally scanned by a combination of the galvanometer mirrors (GMs) and the relay lenses (f = 80 mm and 150 mm, magnification = 1.875). The forward-propagating SHG light was detected by a photon-counting photomultiplier (PMT, Hamamatsu Photonics K. K., H8259-01) after collecting SHG light with a condenser lens and eliminating the laser light with optical filters.

Using the above GM optics, SHG images of a 260 μm by 260 μm region, composed of 256 pixels by 256 pixels, were acquired at a rate of 0.1 image/s. The field of view in SHG imaging is limited by a scanning angle of the galvanometer mirror and/or a magnification factor of the relay lenses. To further enlarge the imaging region, we scanned the sample position horizontally or vertically at intervals of 260 μm using a stepping-motor-driven translation stage every time acquiring an SHG image of 260 μm by 260 μm regions using the GMs. Finally, we obtained a large SHG image with a size of 1.04 mm by 1.04 mm, corresponding to 1024 pixels by 1024 pixels, by stitching 16 SHG images together in a matrix of four rows and four lines.

3. RESULTS

A. Comparison of SHG Images of Cultured-Osteoblasts-Produced Collagen Fibers Obtained with 110 fs and 19 fs Pulsed Light

We visualized the spatial distribution of collagen fibers in a cultured osteoblast sample (culturing period = 3 weeks) by SHG microscopy. Figures 3(a) and 3(b) show a comparison of SHG images of collagen fibers obtained with 110 fs pulsed light (average power = 20 mW) and 19 fs pulsed light (average power = 20 mW), respectively. The gray scales of the SHG light intensity in these two images were corrected by considering the different repetition frequencies (100 MHz for 110 fs pulsed light and 81.8 MHz for 19 fs pulsed light), allowing us to directly compare the intensity of SHG images. The dimness in the edge of the SHG image is mainly due to insufficient filling of water between the objective lens surface and the bottom of the silicone-rubber chamber. In the SHG image obtained with the 110 fs pulsed light, it is difficult to determine the detailed distribution of collagen fibers due to the too low SHG intensity [see Fig. 3(a)]. On the other hand, the SHG image obtained with the 19 fs pulsed light clearly shows that fine collagen fibers were distributed in the whole imaging region, and their density increased locally [see Fig. 3(b)].

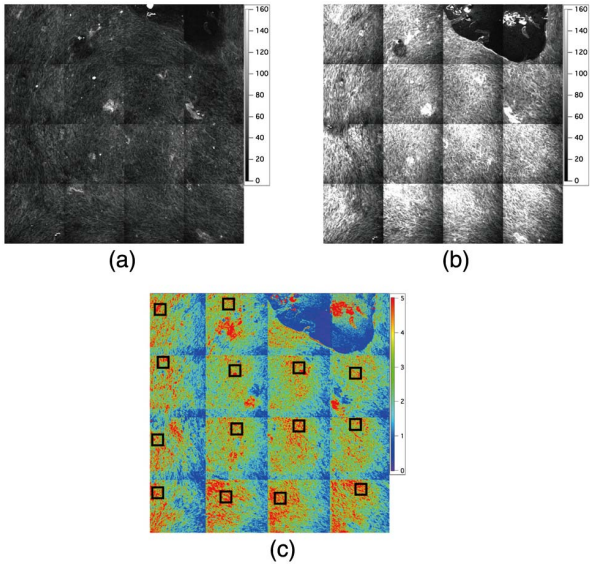

Fig. 3. SHG images of collagen fiber in the cultured osteoblast sample (culturing period = 3 weeks) obtained using (a) 110 fs pulsed light (power = 20 mW) and (b) 19 fs pulsed light (power = 20 mW). Image size is 1040 μm by 1040 μm, composed of 1024 pixels by 1024 pixels. (c) Ratio image obtained by dividing two SHG images obtained with 110 fs pulsed light and 19 fs pulsed light.

Next, to investigate the enhancement of SHG light intensity quantitatively, we generated an image formed by calculating the SHG light intensity ratio at each pixel of the two SHG images in Figs. 3(a) and 3(b). Figure 3(c) shows the resulting ratio image. In 16 regions of interest (ROI) of this ratio image [see black boxes in Fig. 3(c)], the ratios were distributed within 3.81 ± 0.11 (mean ± standard deviation). Since the SHG light intensity has an inverse dependence on the pulse duration under the constant pulse energy [16], an 8.7 times enhancement of the SHG light intensity is expected from the difference in the pulse durations (110 fs and 19 fs). However, the actual enhancement of the SHG image remained as 3.81. One reason for the lower enhancement is in the residual chirping and pedestal components of the 19 fs pulse light. These hardly contribute to SHG light generation due to lower peak power and lead to a decrease in SHG enhancement. Also, the achromatic aberration of the objective lens may have decreased the signal enhancement of the SHG image obtained with 19 fs pulsed light, because the tight focusing of the broadband laser light is a critical factor in SHG microscopy. Nevertheless, the obtained enhancement factor of 3.81 enabled us to visualize the spatial distribution in a thin layer of collagen fibers produced by a single layer of the cultured osteoblasts *in situ* without the need for staining. The risk of photodamage in the cells induced by the ultrashort pulsed light is discussed later.

B. *In Situ* Time-Series SHG Imaging of Collagen Fibers Produced by Standing-Cultured Osteoblasts During 4-Week Culturing Period

We performed *in situ* time-series SHG imaging of the collagen fibers produced in one and the same standing-cultured osteoblast sample. Figures 4(a)–4(e) show time-series SHG images of the collagen fiber distribution in one and the same sample at 0 day, 1 week, 2 weeks, 3 weeks, and 4 weeks, respectively, after starting the standing culture. Although SHG light might be generated from microtubule in the cells in addition to collagen [17], the sample at 0 day, which is before producing the collagen fibers, indicated no SHG signals [see Fig. 4(a)]. Therefore, we can conclude that microtubule did not contribute to the SHG signal in this experiment. In the sample cultured for 1 to 4 weeks, it was clear that the collagen fibers were produced and their distribution changed with the elapsed time. In Fig. 4(b), the distribution of the collagen fibers appeared as circular shapes, implying that the collagen fibers were produced and stored in the osteoblasts. In Fig. 4(c), a similar distribution was confirmed; however, SHG light was more intense than that in Fig. 4(b), implying that the produced collagen fibers accumulated in the osteoblasts and their density increased. In Fig. 4(d), thin collagen fibers appeared as a network structure outside the osteoblasts in addition to the circle-like collagen distribution inside them. In Fig. 4(e), the collagen fibers became thicker, and the density of collagen fibers outside the osteoblasts increased locally. From the comparison of these SHG images with the stained images in Fig. 1, the rough behavior of the collagen fibers during the standing culture was reasonably in agreement between them. However, it should be noted that the SHG images visualized more detailed changes of the collagen fiber distribution than the stained images.

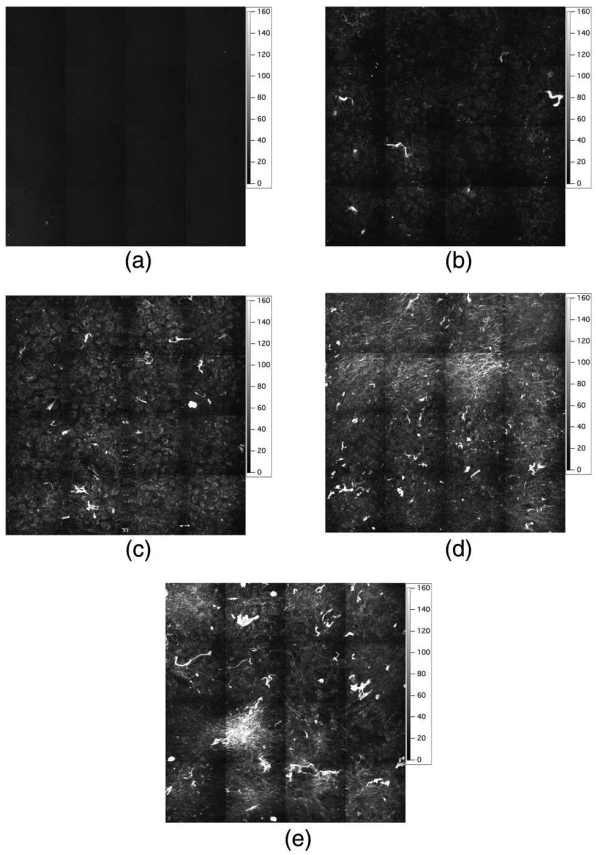

Fig. 4. *In situ* time-series SHG images of collagen fiber distribution produced in one and the same sample of standing-cultured osteoblasts at (a) 0 day, (b) 1 week, (c) 2 weeks, (d) 3 weeks, and (e) 4 weeks after starting the standing culture. Image size is 1040 μm by 1040 μm, composed of 1024 pixels by 1024 pixels.

C. Quantitative Analysis for the Maturity Degree of Collagen Fibers

The characteristic changes in a series of SHG images in Fig. 4 include the accumulation of collagen fibers inside the osteoblasts and the subsequent formation of collagen fiber networks outside the osteoblasts. We consider that such characteristic changes are related to the maturity degree of the collagen fibers. One promising method to extract the spatial characteristics of those SHG images is use of the image analysis based on the 2D-FT [18]. This image analysis is useful for the evaluation of matured native tissues having the specific orientation or the periodic structure of collagen fibers. However, the collagen fibers produced by the cultured osteoblasts are less structured and nonspecifically oriented due to immature structure [see Figs. 4(d) and 4(e)]. To extend the SHG image analysis to the sample with less structured and nonspecifically orientated collagen fibers, we have to use another approach of SHG image analysis. To extract the maturity degree of collagen fibers from SHG image quantitatively, we proposed another 2D-FT-based image analysis and applied it for SHG images in Fig. 4.

We selected a ROI with size of 11 pixels by 11 pixels in the original SHG image (pixel size = 1024 × 1024), calculated the 2D-FT, and obtained the 2D-FT power spectrum. After the curve fitting analysis of the 2D-FT power spectrum with the 2D Gaussian function, we calculated a ratio of a long axis to a short axis (FT-L/S ratio) in the elliptical base of the function. We repeated a similar procedure every time the ROI was shifted horizontally or vertically at 5 pixel intervals, and obtained the 2D mapping of the FT-L/S ratio, namely, an FT-L/S image, with a size of 202 pixels by 202 pixels. The FT-L/S image contains information about the network structure of collagen fibers rather than the density of them because the FT-L/S ratio is not directly related to the SHG light intensity. To take the density of collagen fiber into consideration, we have to convolute the intensity information of the SHG image with the FT-L/S image. To this end, the size of the SHG image was reduced from 1024 pixels by 1024 pixels to 202 pixels by 202 pixels by binning the data in each ROI, and the resized SHG image was multiplied by the FT-L/S image. The resulting image includes information on both the network structure and the density of collagen fibers. We called this image a collagen maturity factor (CMF) image. After segmenting the CMF image (pixel size = 202 × 202) into 16 images (pixel size = 50 × 50), we calculated the mean CMF value for each segmented image. Finally, we performed the significance test of the mean CMF values among the samples cultured for different periods.

Figure 5 shows the comparison of the original SHG image, the FT-L/S image, the resized SHG image, and the CMF image

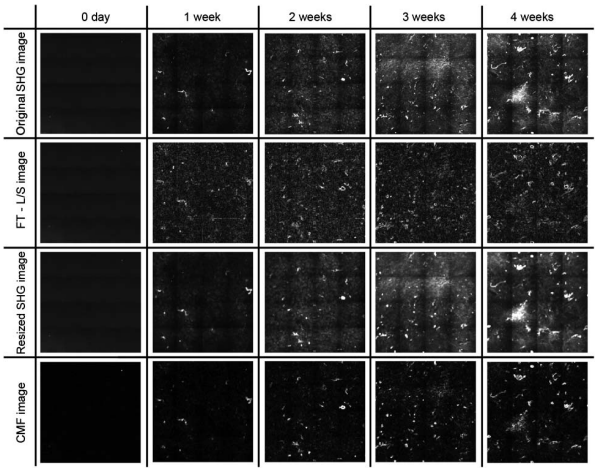

Fig. 5. Comparison of the original SHG image (1024 pixels by 1024 pixels), the FT-L/S image (202 pixels by 202 pixels), the resized SHG image (202 pixels by 202 pixels), and the CMF image (202 pixels by 202 pixels) with respect to the elapsed time of the standing culture.

with respect to the elapsed time of the standing culture. We consider that the CMF image reasonably reflected the temporal evolution of the collagen fibers, or the maturity degree of collagen fibers, during the standing culture.

Figure 6 shows the relation between the culturing periods and the mean CMF values for 16 segmented CMF images, indicating the increase of the mean CMF value with respect to the elapsed time. There were significant differences among the samples cultured for 0 day, 1 week, 2 weeks, and 3 weeks. On the other hand, no significant difference between samples cultured for 3 weeks and 4 weeks may imply nearly saturation of the collagen production during the standing culture.

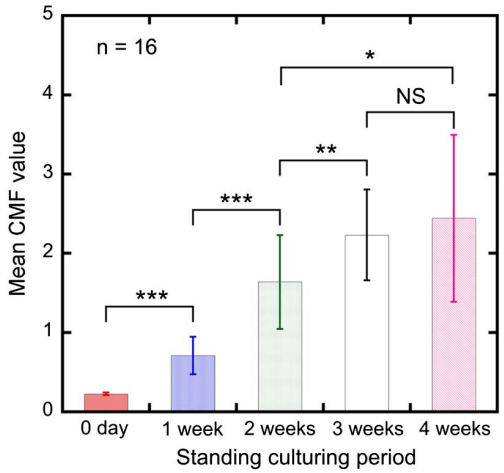

Fig. 6. Relation between the culturing periods and the mean CMF value for 16 segmented CMF images. The p value was calculated by Student's t-test (*, $p < 0.05$; **, $p < 0.01$; ***, $p < 0.001$; NS, not significant).

4. DISCUSSION

We succeeded in demonstrating *in situ* time-series SHG imaging of the collagen fibers produced by standing-cultured osteoblasts. Use of the 19 fs pulsed light enables sensitive visualization of the thin-layer collagen fibers produced by a single layer of the osteoblasts; however, we could not visualize it at high image contrast by use of the 110 fs pulsed light. Such sensitive SHG imaging of osteoblast-produced collagen fibers will open a new door for bone tissue engineering and regeneration. First, the specific selectivity to only collagen fibers, with high image contrast, allows simple and straightforward investigation of the collagen dynamics in cultured osteoblast samples. The high-contrast, background-free SHG images make the image analysis more powerful for quantitative analysis. It is in contrast to the stained procedure where not only the collagen fibers but also the osteoblasts were stained with the similar pink color. Second, and more importantly, the stain-free visualization of collagen fibers allows us to *in situ* monitor one and the same sample in a time series. This feature is useful for determining the response of collagen fibers to various external stimuli as well as the standing culture. For example, it is known that a mechanical stimulus [19] or chemical one [20] promotes the production of collagen fibers by cultured osteoblasts. Furthermore, to achieve the desired mechanical properties of bone tissue, it may be possible to control the production, superorganization, and/or orientation of collagen fibers in bone tissue by stimulus feedback based on the monitoring of SHG images. This method will open the door for *in situ* feedback control of the quality and quantity in collagen fibers in bone tissue engineering.

Next, we consider the relation between the collagen maturity degree and the start of the bone mineralization because osteoblasts create the nanocomposite structure of bone by secreting a collagenous extracellular matrix on which apatite crystals subsequently form [21]. Figures 7(a)–7(c) show the phase contrast image of the standing-cultured osteoblast samples at 7 days, 21 days, and 31 days after starting the culture,

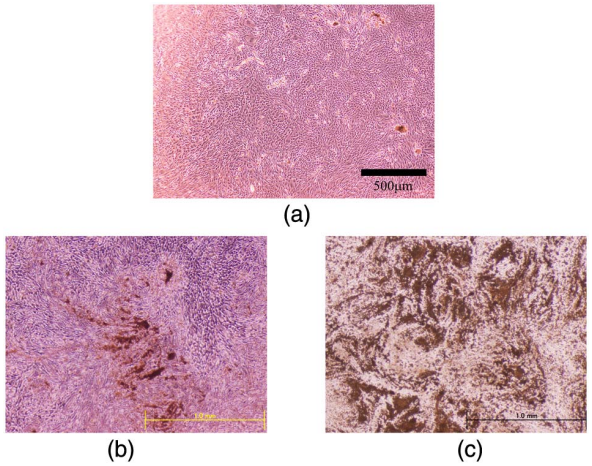

Fig. 7. Phase contrast image of the standing-cultured osteoblast samples at (a) 7 days, (b) 21 days, and (c) 31 days after starting the culture, respectively. The black parts indicate the apatite crystals and the pink color is mainly due to the culture medium.

respectively. The black parts in these images indicate the apatite crystals and the pink color is mainly due to the culture medium. In Fig. 7(a), the osteoblasts proliferated and became confluent, whereas the apatite crystals did not form yet. After that, the apatite crystals started to appear [see Fig. 7(b)] and increased their area with the lapse of time [see Fig. 7(c)]. These temporal behaviors of the apatite crystals were significantly in accord with the saturation of collagen production, or the collagen maturity, indicated by the mean CMF value in Fig. 6. Therefore, the mean CMF value may be used as an indicator for the start of bone mineralization during the culture.

While use of the sub-20 fs pulsed light effectively enhanced the image contrast in the SHG microscopy of the skin tissue [22] and the fibroblast-produced collagen fibers [13] in addition to the osteoblast-produced collagen fibers in this study, we may have to consider its invasiveness to cells. When reducing the pulse duration below 100 fs, the high peak energy increases the risk of nonlinear photodamage and decreases the viability of living cells. For example, in the previous study for the Chinese hamster ovarian cell, the risk of the photodamage in multiphoton microscopy increased inversely proportional to the pulse duration [23]. Also, a similar result was obtained in bovine adrenal chromaffin cells [24]. However, there have been no attempts to investigate the photodamage of the osteoblasts. During the culturing period of 4 weeks in Fig. 4, we monitored the morphological change of the osteoblasts using the phase contrast microscopy together with SHG microscopy. However, we did not observe the structural change of them (not shown). Furthermore, SHG images in Fig. 4 indicate that the laser-beam-irradiated osteoblasts adequately produced collagen fibers during the culturing period in the same manner as the osteoblasts without irradiation of the laser beam (not shown). However, these are no more than the preliminary findings about the photodamage. The more careful analysis of the photodamage is required to conclude whether the osteoblasts are photodamaged or not. Future work is to quantitatively investigate the influence of the laser irradiation on the osteoblast by measuring alkaline phosphatase activity, which is a marker of bone production activity [25].

5. CONCLUSIONS

We constructed a SHG microscope for *in situ* time-series monitoring of collagen fibers produced by standing-cultured osteoblasts. Use of the 19 fs pulsed light enables us to visualize a thin layer of collagen fibers produced by a single layer of the osteoblasts in high-contrast SHG images. Using this SHG microscope, the temporal evolution of the collagen fiber distribution in the standing-cultured osteoblast samples was continuously monitored during a culturing period of 4 weeks in the form of high-contrast, time-series SHG images. From a comparison with the staining procedure, we confirmed the ability to obtain knowledge about the detailed behavior of collagen fibers during the culturing period from the SHG images. Furthermore, we succeeded in extracting a quantitative parameter of the collagen maturity degree in the cultured sample by use of the image analysis based on 2D-FT of SHG images. Although 2D SHG imaging was performed in this paper, 3D imaging capability in SHG microscopy will be useful for volume evaluation of the osteoblast-produced collagen fibers if the 3D culturing model of osteoblasts is prepared by use of collagen gel or scaffold. Such *in situ* visualization and the quantitative analysis of the osteoblast-produced collagen fibers will be a powerful tool for the quality control of cultured and/or regenerated tissues in bone tissue engineering.

Funding. Ministry of Education, Culture, Sports, Science, and Technology (MEXT) (25560200); Tokushima University.

Acknowledgment. The authors are grateful to Dr. S. Fukushima of Osaka University for fruitful discussions.

REFERENCES

1. A. J. Salgado, O. P. Coutinho, and R. L. Reis, "Bone tissue engineering: state of the art and future trends," Macromol. Biosci. **4**, 743–765 (2004).
2. K. E. Healy and R. E. Guldberg, "Bone tissue engineering," J. Musculoskelet. Neuronal Interact. **7**, 328–330 (2007).
3. K. Kanke, H. Masaki, T. Saito, Y. Komiyama, H. Hojo, H. Nakauchi, A. C. Lichtler, T. Takao, U. Chung, and S. Ohba, "Stepwise differentiation of pluripotent stem cells into osteoblasts using four small molecules under serum-free and feeder-free conditions," Stem Cell Rep. **2**, 751–760 (2014).
4. J.-H. Hong, E. S. Hwang, M. T. McManus, A. Amsterdam, Y. Tian, R. Kalmukova, E. Mueller, T. Benjamin, B. M. Spiegelman, P. A. Sharp, N. Hopkins, and M. B. Yaffe, "TAZ, a transcriptional modulator of mesenchymal stem cell differentiation," Science **309**, 1074–1078 (2005).
5. L. E. Smith, R. Smallwood, and S. MacNeil, "A comparison of imaging methodologies for 3D tissue engineering," Microsc. Res. Tech. **73**, 1123–1133 (2010).
6. P. J. Campagnola and C. Y. Dong, "Second harmonic generation microscopy: principles and applications to disease diagnosis," Laser Photon. Rev. **5**, 13–26 (2011).
7. T. Yasui, Y. Takahashi, S. Fukushima, and T. Araki, "*Ex vivo* and *in vivo* second-harmonic-generation imaging of dermal collagen fiber in skin: comparison of imaging characteristics between mode-locked Cr:forsterite and Ti:sapphire lasers," Appl. Opt. **48**, D88–D95 (2009).
8. R. M. Williams, W. R. Zipfel, and W. W. Webb, "Interpreting second-harmonic generation images of collagen I fibrils," Biophys. J. **88**, 1377–1386 (2005).
9. H.-Y. Tan, S. W. Teng, W. Lo, W. C. Lin, S. J. Lin, S. H. Jee, and C. Y. Dong, "Characterizing the thermally induced structural changes to intact porcine eye, part 1: second harmonic generation imaging of cornea stroma," J. Biomed. Opt. **10**, 054019 (2005).
10. W. R. Zipfel, R. M. Williams, R. Christie, A. Y. Nikitin, B. T. Hyman, and W. W. Webb, "Live tissue intrinsic emission microscopy using multiphoton-excited native fluorescence and second harmonic generation," Proc. Natl. Acad. Sci. USA **100**, 7075–7080 (2003).
11. J. C. Mansfield, C. P. Winlove, J. Moger, and S. J. Matcher, "Collagen fiber arrangement in normal and diseased cartilage studied by polarization sensitive nonlinear microscopy," J. Biomed. Opt. **13**, 044020 (2008).
12. L. Mortati, C. Divieto, and M. P. Sassi, "CARS and SHG microscopy to follow collagen production in living human corneal fibroblasts and mesenchymal stem cells in fibrin hydrogel 3D cultures," J. Raman Spectrosc. **43**, 675–680 (2012).
13. J. J. Hu, J. D. Humphrey, and A. T. Yeh, "Characterization of engineered tissue development under biaxial stretch using nonlinear optical microscopy," Tissue Eng. Part A **15**, 1553–1564 (2009).
14. H. Tullberg-Reinert and G. Jundt, "*In situ* measurement of collagen synthesis by human bone cells with a Sirius Red-based colorimetric microassay: effects of transforming growth factor β2 and ascorbic acid 2-phosphate," Histochem. Cell Biol. **112**, 271–276 (1999).
15. J. B. Guild, C. Xu, and W. W. Webb, "Measurement of group delay dispersion of high numerical aperture objective lenses using two-photon excited fluorescence," Appl. Opt. **36**, 397–401 (1997).

16. P. J. Campagnola, H. A. Clark, W. A. Mohler, A. Lewis, and L. M. Loew, "Second-harmonic imaging microscopy of living cells," J. Biomed. Opt. **6**, 277–286 (2001).
17. P. J. Campagnola, A. C. Millard, M. Terasaki, P. E. Hoppe, C. J. Malone, and W. A. Mohler, "Three-dimensional high-resolution second-harmonic generation imaging of endogenous structural proteins in biological tissues," Biophys. J. **82**, 493–508 (2002).
18. R. A. Rao, M. R. Mehta, and K. C. Toussaint, "Fourier transform-second-harmonic generation imaging of biological tissues," Opt. Express **17**, 14534–14542 (2009).
19. A. Matsugaki, N. Fujiwara, and T. Nakano, "Continuous cyclic stretch induces osteoblast alignment and formation of anisotropic collagen fiber matrix," Acta Biomater. **9**, 7227–7235 (2013).
20. W. N. Addison, "Extracellular matrix mineralization in murine MC3T3-E1 osteoblast cultures: an ultrastructural, compositional and comparative analysis with mouse bone," Bone **71**, 244–256 (2015).
21. S. Boonrungsimane, E. Gentleman, R. Carzaniga, N. D. Evans, D. W. McComb, A. E. Porter, and M. M. Stevens, "The role of intracellular calcium phosphate in osteoblast-mediated bone apatite formation," Proc. Natl. Acad. Sci. USA **109**, 14170–14175 (2012).
22. S. Tang, T. B. Krasieva, Z. Chen, G. Tempea, and B. J. Tromberg, "Effect of pulse duration on two-photon excited fluorescence and second harmonic generation in nonlinear optical microscopy," J. Biomed. Opt. **11**, 020501 (2006).
23. K. König, T. W. Becker, P. Fischer, I. Riemann, and K. J. Halbhuberet, "Pulse-length dependence of cellular response to intense near-infrared laser pulses in multiphoton microscopes," Opt. Lett. **24**, 113–115 (1999).
24. A. Hopt and E. Neher, "Highly nonlinear photodamage in two-photon fluorescence microscopy," Biophys. J. **80**, 2029–2036 (2001).
25. H. Sudo, H. A. Kodama, Y. Amagai, S. Yamamoto, and S. Kasai, "Establishment of a clonal osteogenic cell line from newborn mouse calvaria," Jpn. J. Oral Biol. **23**, 899–901 (1981).